Title: Reduced Graphene Oxide Membranes in Ocular Regenerative Medicine

Authors: Iriana Zambrano-Andazol[1], Natalia Vázquez[1], Manuel Chacón[1], Ronald M. Sánchez-Avila[1], Mairobi Persinal[1], Clara Blanco[2], Zoraida González[2], Rosa Menéndez[2], María Sierra[3], Álvaro Fernández-Vega[1], Teresa Sánchez[4], Jesús Merayo-Lloves[1], Álvaro Meana[1].

Place of work:

[1]Instituto Universitario Fernández-Vega. Fundación de Investigación Oftalmológica. Universidad de Oviedo (Asturias, Spain); [2]Instituto de Ciencia y tecnología del Carbono, INCAR-CSIC (Asturias, Spain); [3]Departamento de Biología Funcional. Área de Genética. Universidad de Oviedo. (Asturias, Spain); [4]Unidad de Bioterio e Imagen Preclínica. Universidad de Oviedo (Asturias, Spain).

Offprint requests to: Álvaro Meana. Instituto Universitario Fernández-Vega. Avda. Dres. Fernández-Vega, 34. 33012. Oviedo, Asturias, Spain. E-mail: meana@fio.as.

Abstract

Biological membranes are currently used in Ophthalmology in order to treat different ocular disorders. These membranes have different properties such as cellular biocompatibility and promoting wound healing. Moreover, intrinsic antimicrobial properties could also be desirable because it would allow their use reducing the risk of infections.

Graphene and its derivatives are promising biomaterials that already proved their bactericidal effect. However, their clinical use is limited due to the controversial results regarding their toxicity. In this work, we have developed and characterized a reduced graphene oxide membrane (rGOM) for its use in ocular Regenerative Medicine, and studied its *in vitro* and *in vivo* biocompatibility and genotoxicity with different types of human ocular cells.

We proved that rGOM allowed the growth of different ocular cells without inducing *in vitro* or *in vivo* cytotoxicity or genotoxicity in the short-term. These results indicate that rGOM may be a promising candidate in Regenerative Medicine for the treatment of different ocular pathologies.

Keywords: Reduced graphene oxide membrane, GO biocompatibility, ocular Regenerative Medicine, Tissue Engineering, Ophthalmology.

Funding: This work was supported by Consejería de Economía y Empleo del Principado de Asturias: [grant number: IDE/2014/000737 and IDE/2015/000889].

1. Introduction

Graphene and its derivatives have increased their interest in various industrial and scientific fields due to their unique mechanical, thermal and electronic properties [1–4]. Graphene based materials have been studied for manufacturing radio frequency identification antennas [5], lithium-ion batteries [6], sensors [7] and photovoltaic cells [8], in electronics, aeronautics and automotive industries. In recent years, the interest in graphene-based materials has been translated into biological and biomedical applications, and graphene

derivatives have been analyzed as biosensors [9,10], diagnostic tools [11], in drug-delivery studies [12,13] and Regenerative Medicine [14].

Graphene oxide (GO) is the most promising of all graphene-based materials for use in biological and biomedical applications due to its high solubility in water and many other polar solvents, and the presence of oxygenated functional groups [9,12,15,16]. Moreover, GO shows great antibacterial properties against a wide variety of microorganisms, including Gram-positive and Gram–negative bacterial pathogens, phytopathogens and biofilm forming microorganisms [17–20].

Obtaining GO from natural graphite, involves chemical, thermal and/or mechanical procedures [21–23]. Depending on these procedures, the final GO obtained may vary in the sheet size and in the type and location of oxygenated functional groups [24], which can influence on its toxicity [25]. Several studies indicate that GO is a highly biocompatible material that allows the adhesion and proliferation of different cell lines with limited or no cytotoxicity [26–29]. In contrast, other studies have demonstrated that graphene derivatives generate oxidative reactive species which leads to cytotoxicity [30–33]. All these facts make controversial the use of GO as biomaterial in biomedical applications.

In Ophthalmology, several biological membranes are used during surgery and Tissue Engineering procedures in four main areas: the ocular surface, the corneal endothelium, glaucoma and the retina. Amniotic membrane is employed for repairing ocular surface in the treatment of infections, ocular burns or when there is a risk of ocular perforation [34,35]. Amniotic membrane and fibrin derived membranes are also used as scaffold to culture epithelial limbal stem cells for the treatment of limbal stem cell deficiency [36,37]. Other biological membranes as collagen membranes, have been employed as scaffold for corneal endothelial tissue engineering [38,39]. Finally, donor sclera membranes are used as patch graft material in glaucoma drainage device surgery [40] and fibrin-derived platelet membranes are used as a covering for macular holes [41,42], a type of severe retinal disease with a poor prognosis and requiring surgical treatment.

Graphene-based materials, with their unique properties, have been used in eye-related biomedical applications (contact lens [43–45]**,** keratoprosthesis [46] and bio-subretinal chip [47]). Such direct eye-contact requires many eye-toxicity studies of graphene and graphene derivatives, guaranteeing high safety standards for patients. Several studies have demonstrated a good graphene or GO biocompatibility *in vitro* with different ocular cells, and *in vivo* when the material was directly exposed to ocular structures [48–50]. However, other studies have shown GO cytotoxicity in a time- and dose-dependent way [51] and more recently, a study has demonstrated that short-term repeated GO exposure can cause *in vitro* and *in vivo* toxicity, while reduced GO (rGO) did not cause significant ocular toxicity in mice [52].

Graphene-based scaffolds are used for Tissue Engineering of heart, bone, cartilage, nerve, skin and liver [53,54] but, to our knowledge, there are no studies regarding the use of graphene membranes in ocular Regenerative Medicine. Due to their advantageous properties, in particular their antibacterial activity [20], graphene membranes may be promising

candidates for their application in ocular Regenerative Medicine if their safety is demonstrated.

In this work, we have developed and characterized a reduced GO membrane (rGOM) for its use in ocular Regenerative Medicine. We have also studied the *in vitro* biocompatibility and genotoxicity of rGOM with different types of human ocular cells and its response and integration *in vivo,* demonstrating that rGOM has good biocompatibility without associated cytotoxicity or genotoxicity. All these facts make rGOM a promising candidate for the treatment of different ocular pathologies.

2. Materials and Methods

2.1. Preparation and characterization of GO water suspension.

2.1.1. Preparation of GO water suspension.

GO was obtained from commercial graphite (powder, <20 µm, Sigma-Aldrich, Saint Louis, Missouri, USA) by following a modified Hummer´s method [21]. Briefly, concentrated H_2SO_4 (360 mL, Sigma-Aldrich) was added to a mixture of graphite (7.5 g of powder, <20 µm) and $NaNO_3$ (Scharlab, Barcelona, Cataluña, Spain). The mixture was cooled down to 0°C in an ice bath. $KMnO_4$ (45 g, Sigma-Aldrich) was added slowly in small doses to keep the reaction temperature below 20°C. The solution was then heated to 35°C and stirred for 3 h. After this period of time 3 % of H_2O_2 (1.5 L, Scharlab) was slowly added, giving rise to a pronounced exothermal effect. The reaction mixture was stirred for 30 min and then centrifuged (2,100 rcf for 30 min), after which the supernatant was discarded. The remaining solid material was washed with 600 mL of water and centrifuged. This process was repeated until a neutral pH was achieved. At this point, the obtained GO powder was dispersed in a water solution and exfoliated into GO sheets by ultrasonication (Bransonic Ultrasonic 5510-MTH, 135 W- 42 KHz, Branson, Danbury, Connecticut, USA) for 8 h to obtain GO.

2.1.2. Characterization of GO water suspension.

The GO sheets were imaged using an atomic force microscope (AFM) (Cervantes atomic force microscope, Nanotec Electronica™ Madrid, Spain) operating under ambient conditions (20°C and 80 % relative humidity) in order to measure their lateral size and height. The data were processed using WSxM software (Nanotec Electronica™). AFM samples were prepared by placing two drops of the previously prepared GO water suspension on a mica substrate and leaving them to dry for one day. Nanosensor™ PPP-NCH PointProbe® Plus micro-cantilevers (Nanotec Electronica™, Madrid, Spain) were used to image the GO sheets via the attractive regime amplitude-modulated imaging mode to ensure that the sheets would not be deformed by the microcantilever tip. The flooding option of the WSxM software was employed to visualize the sheets. The areas of the samples were obtained by measuring the lateral size in two planar directions and assuming that each sheet had either a quadrilateral or triangular shape.

2.2. Preparation and characterization of rGOM.

2.2.1. Preparation of rGOM.

Firstly, an amount of 2 mg/cm^2 of GO water suspension was casted onto a silicone mold (Ø=3 cm) and air-dried at room temperature for 24 h, in a laminar air flow cabinet, to obtain a GO membrane. In a second step, the GO membrane was subjected to a chemical reduction procedure by treating it with 3 mL of hydroioidic acid (HI) at 57 wt% (ACROS Organics, Morris Plains, New Jersey, USA) for 6 h. The rGOM were finally washed in phosphate buffered saline (PBS) and stored in the same buffer at room temperature until its use.

2.2.2. Characterization of rGOM.

The surface morphology of the rGOM (N=2) was studied by scanning electron microscopy (SEM). Samples were analyzed using a JEOL-6610LV instrument operating at 25 KV, (JEOL, Akishima, Tokyo, Japan). This microscope was also fitted with an energy dispersive X-ray (EDX) analyzer to allow the detection and quantification of elements present in three 1 mm^2 randomly selected regions of the produced rGOM (GO membranes were also measured for comparative purposes). Furthermore, the atomic content on the surface was determined by XPS analysis in a VG-Microtech Multilab 3000 spectrometer (SPECS, Berlin, Germany) equipped with a hemispherical electron analyzer and a MgKα (hυ = 1253.6 eV) X-ray source. At this point the rGOM was previously pre-treated (thermal treatment) in order to remove the iodine content which could damage the analyzer.

The electrical conductivity (σ) of both the GO and rGOM (N=3) was calculated from direct measurements of their corresponding resistances (R). For this purpose, a dual display multimeter (Fluke, Glenwood, Illinois, USA) equipped with two probes separated by 1 cm (l) was used to do repetitive measurements (N=5). The average value of σ was then estimated by using the following equation:

$$\sigma = R^{-1} S^{-1} l$$

Where S is the cross-section of the membranes investigated (3.0 x 10^{-9} m^2).

The mechanical properties of the rGOM were tested on 5 different membranes with a TA. TXplus texture analyzer (Stable Micro Systems, Godalming, Surrey, UK) with a 5 mm diameter SMS P/5 S spherical probe in order to obtain the burst strength (g) and the distance at burst (mm).

Statistical analyses were performed using IBM SPSS software (IBM Analytics, Armonk, New York, USA). Significant differences among defined groups were tested using the t-student test. A difference level of $p<0.05$ was considered as statistically significant.

2.3. *In vitro* biocompatibility of rGOM.

The study of the *in vitro* biocompatibility of rGOM was performed using 2 human ocular cell lines and 3 types of human primary ocular cells which were cultured on 2 cm^2 rGOM. rGOM was not subjected to any sterilization protocol prior to cell culture techniques.

2.3.1. Culture of human ocular cells lines.

The human retinal pigment epithelial cell line (ARPE-19) was kindly provided by BTI Biotechnology Institute (Vitoria, País Vasco, Spain) and the human corneal epithelial cell line

(HCE-T) was obtained from RIKEN Bioresource Research Center (Tsukuba, Ibaraki, Japan). Both cell lines were expanded in accordance with their ATCC specifications.

ARPE-19 cells were cultured in a 1:1 mixture of Dulbecco Modified Eagle`s Medium and Ham's F12 (DMEM/F12) culture medium supplemented with 10 v/v% fetal bovine serum (FBS), 100 U/mL penicillin and 0.1 mg/mL streptomycin (Sigma-Aldrich). HCE-T cells were cultured in a 1:1 mixture of DMEM/F12 culture medium supplemented with 5 v/v% FBS, 100 U/mL penicillin and 0.1 mg/mL streptomycin, 5 µg/mL insulin (Sigma-Aldrich) and 5 ng/mL epidermal growth factor (Austral Biologicals, San Ramon, California, USA).

Confluent cultures of ARPE-19 and HCE-T between passage 8 and 20 were trypsinized with trypsin/EDTA 0.25 % (Sigma-Aldrich), centrifuged, and reseeded at a density of 100,000 cells/cm^2 in rGOM and 24-well culture plates as control group.

2.3.2. Primary culture of human ocular cells.

Human tissue was handled according to the Declaration of Helsinki. Eyeballs and corneoscleral rings from corneas previously used for penetrating keratoplasty were obtained from the local Eye Bank (Centro Comunitario de Sangre y Tejidos, Oviedo, Asturias, Spain) and the Instituto Oftalmológico Fernández-Vega (Oviedo, Asturias, Spain) respectively. All tissues were maintained at 4°C in Eusol-C storage medium (Alchimia, Ponte San Nicolò, Padova, Italy) for less than 10 days before use.

2.3.2.1. Culture of primary human corneal keratocytes.

Primary human corneal keratocytes were cultured in 1:1 mixture of DMEM/F12 culture medium supplemented with 10 v/v% FBS, 100 U/mL penicillin and 0.1 mg/mL streptomycin, 1 v/v% non-essential amino acid solution and 1 v/v% RPMI 1640 vitamin solution (Sigma-Aldrich).

The stromal region was dissected, cut into small pieces and digested with trypsin/EDTA 0.25 % for 30 min at 37°C. After that, the trypsin was neutralized with culture medium. The detached cells were centrifuged using an Eppendorf 5702R centrifuge (Eppendorf, Hamburg, Germany) at 400 rcf for 10 min and the supernatant was discarded. Fresh medium was added and the cells were seeded on a culture plate. Once the cultures were confluent, cells were trypsinized, centrifuged and reseeded at a density of 100,000 cells/cm^2 on rGOM and 24-well culture plates as control group.

2.3.2.2. Culture of primary human corneal limbal cells.

Primary human corneal limbal cells were cultured in 2:1 mixture of DMEM/F12 culture medium supplemented with 10 v/v% FBS, 100 U/mL penicillin and 0.1 mg/mL streptomycin, 24 µg/mL adenine, 5 µg/mL insulin, 8.33 ng/mL cholera toxin, 1.3 ng/mL triiodothyronine and 0.4 µg/mL hydrocortisone (Sigma-Aldrich). This medium was used in the first 3 days of culture. After that, cells were cultured in the same medium with 10 ng/mL of epidermal growth factor.

Cells were cultured from limbal explants in the absence of feeder cells. Sclerocorneal limbus was dissected under a microscope, cut in 2 mm^3 fragments, placed on rGOM and covered with culture medium. Explants were placed on 24-well culture plates as control group.

2.3.2.3. Culture of primary human retinal pigment epithelial cells (RPE).

Primary RPE cells were cultured in 2:1 mixture of DMEM/F12 culture medium supplemented with 15 v/v% FBS, 100 U/mL penicillin and 0.1 mg/mL streptomycin, 10 mM non-essential amino acid solution, 0.093 ng/mL triiodothyronine, 0.02 µg/mL hydrocortisone, 1X N1 supplement, 2 mM L-glutamine and 0.25 mg/mL taurine (Sigma-Aldrich).

RPE cultures were obtained according to a protocol described elsewhere [42], with some modifications. Briefly, cadaver donor eyeballs obtained within 24-36 h postmortem were dissected, the vitreous and retina were removed, and the posterior eye-cup rinsed with PBS, and then incubated in 1 % dispase (Thermo Fisher Scientific, Waltham, Massachusetts, USA) for 45 min at 37°C. The RPE was gently scraped off Bruch's membrane and placed in DMEM/F12 supplemented with 10 % FBS and with 10 % sucrose (VWR, Radnor, Pennsylvania, USA). After 30 min, the lower fraction containing RPE was collected, centrifuged at 300 rcf for 5 min, resuspended in DMEM/F12 supplemented with 15 % FBS, and plated in Matrigel coated culture plates (Corning® Matrigel® Basement Membrane Matrix, Discovery Labware, Inc. Bedford, Massachusetts, USA). RPE cells attached and grew to confluence while decreasing progressively the percentage of FBS to reach 2 % in 2-3 weeks. At that time, cells were trypsinized, centrifuged and reseeded (1:2) on rGOM and 24-well culture plates as control group.

All cultures were maintained in a humidified incubator at 37°C with 5 % CO_2, and the medium was changed twice a week.

2.3.3. Characterization of human ocular cell cultures.

Cellular growth in the control group was assessed using a Leica DMIL LED phase contrast microscope (Leica, Wetzlar, Hesse, Germany) and photos were taken with an attached EC3 camera (Leica). Once the cultures in the control group were confluent, rGOM cultured with ocular cells and control cultures were fixed with ice cold methanol (Sigma-Aldrich) for 10 min and used for immunocytochemical characterization and SEM.

For immunocytochemistry studies, methanol fixed cultures were rinsed twice with PBS for 5 min and permeabilized in PBS containing 0.3 % Triton-X100 (VWR) for another 5 min. Next, the samples were rinsed again with PBS once for 5 min and incubated with primary antibodies containing 10 % normal goat serum (Catalog number: ab7481, Abcam, Cambridge, UK) as a blocking agent at 4°C overnight. Vimentin (1:100; Catalog number: M0725, Agilent DAKO, Santa Clara, California, USA) antibody was used to identify corneal keratocytes. Cytokeratin high molecular weight (CK) (1:40; Catalog number: M0630, Agilent DAKO) and p63 (1:100; Catalog number: ab124762, Abcam) antibodies were used to identify corneal limbal cells. RPE65 (1:100; Catalog number: MA1-16578, Thermo Fisher Scientific) and zonula occludens-1 (ZO-1) (1:100; Catalog number: 61-7300, Thermo Fisher Scientific) antibodies were used to identify RPE and ARPE-19. E-cadherin (1:200; Catalog number: sc-7870, Santa Cruz

Biotechnology, Dallas, Texas, USA) and CK (1:40) antibodies were used to identify HCE-T. Subsequently, the samples were incubated with secondary antibodies (1:500; Catalog number: A-11032 and A-11034, Thermo Fisher Scientific) for 2 h at room temperature. Between the incubation steps the cells were washed three times with PBS for 5 min. Immunolabeled cells were stained with 4´, 6-diamidino-2-phenylindole (DAPI) (Thermo Fisher Scientific) to allow nuclei visualization. All the samples were examined using a Leica DM6000B fluorescence microscope (Leica).

Finally, the surface morphology of fixed rGOM cultured with ocular cells was observed under SEM. For this purpose, fixed rGOM was subjected to a dehydration process through a graded series (30, 50, 70, 90 and 100 %) of acetone (Thermo Fisher Scientific) for 10 min and dried by the critical-point method. Cells were visualized in a JEOL 6610LV SEM microscope at 25 KV of accelerated voltage.

2.4. *In vitro* genotoxicity assay.

The possible genotoxicity effect of the rGOM on ocular cells was analyzed using the comet assay (single-cell gel electrophoresis) for detection of strand breaks [55] in corneal keratocytes and ARPE-19 cells cultured on rGOM. The experiment was performed in triplicate for each cell type.

After 48 h of culture on the rGOM, cells were detached with trypsin/EDTA 0.25 % for 10 min at 37°C. After that, the trypsin was neutralized with culture medium. The detached cells were centrifuged at 400 rcf for 10 min and the supernatant was removed. The pellet was resuspended in PBS at 10^6 cells/mL and 30 µL of those cell suspensions were mixed with 65 µL of low melting point agarose (Thermo Fisher Scientific) at 37°C, to reach a final 0.5 % agarose concentration. The solution was placed on 0.5 % normal melting point agarose precoated slides and incubated for 1 h in lysis solution (2.5 M NaCl, 0.2 M NaOH, 100 mM Na_2EDTA, 10 mM Tris-HCL, 10 % DMSO and 1 % Triton-X100, pH=10, Sigma-Aldrich) at 4°C and darkness. Afterwards, the slides were placed on an electrophoresis tank and were incubated with denaturing/electrophoresis buffer (300 mM NaOH, 1 mM EDTA, pH>13) for 20 min and electrophoresed at 0.93 V/cm for 20 min. Then, they were neutralized, rinsed 3 times with PBS for 5 min and fixed with absolute ethanol (Sigma-Aldrich), for 3 min. After drying at room temperature overnight, slides were stained with 40 µL of dye solution (0.5 µg/mL ethidium bromide, Sigma-Aldrich) and 1 µL of fluorescence protector Vectashield® (VECTOR laboratories, Burlingame, California, USA), covered with coverslips and visualized with an Olympus BX-61 fluorescence microscope with digital camera DP-70 (Olympus Optical, Shinjuku, Tokyo, Japan). For each experiment, two slides were prepared for each cell type, and 50 random field images were analyzed using the KOMET 5 program (Kinetic, Liverpool, UK). The results were expressed as percentage of tail DNA.

Statistical analyses were performed using IBM SPSS software. Significant differences among defined groups were tested using the t-student test. A difference level of $p<0.05$ was considered as statistically significant.

2.5. *In vivo* biocompatibility of rGOM.

The protocols for the study of *in vivo* biocompatibility were approved (PROAE 29/2016) by the Committee on the Ethics of Animal Experiments of the University of Oviedo and the Animal Production and Health Service of Asturias and were performed following the European Directive 2010/63/EU for animal experiments.

In vivo biocompatibility of the rGOM was examined in 12 Wistar rats (2 months of age males and body weight of approximately 200 g) obtained from the Animal Housing Facility of the University of Oviedo (Oviedo, Asturias, Spain). Rats were kept under a 12/12 day/night light cycle with food and water *ad libitum* and were monitored on a daily basis.

Wistar rats were divided in two groups (7 and 21 days) and subdivided in two subgroups: rats with or without rGOM (control group). Animals were firstly anesthetized by an intraperitoneal injection of ketamine (80 mg/kg, Richter Pharma, Wells, Austria) and xylazine (10 mg/kg, Bayer, Leverkusen, Germany) and a 1 cm incision was made on the back of the rats. Then, rGOM (Ø=0.5 cm) were implanted into subcutaneous tissue. The wounds were closed with 5-0 nylon non-absorbable sutures.

After the established times, Wistar rats were euthanized by an intravenous overdose of pentobarbital sodium (Vetoquinol, Madrid, Spain). Then, rGOM and the surrounding tissue was dissected and fixed for 4 h in Somogyi (4 % paraformaldehyde solution containing 0.2 % picric acid in PBS 0.1 M pH 7.4, Sigma-Aldrich), embedded in paraffin, sectioned and stained with haematoxylin-eosin (H/E) (Sigma-Aldrich) and analyzed under light microscopy.

Additionally, biocompatibility was also evaluated in 4 New Zealand white rabbits. Rabbits were divided in two groups. The first group (N=2) were transplanted with intrastromal rGOM and the second group (N=2) were transplanted with intrascleral rGOM.

Briefly, rabbits were anesthetized with Bupaq® (0.01-0.05 mg/kg buprenorphine, Richter Pharma) and Metacam® (0.3 mg/kg meloxicam, Boehringer Ingelheim, Ingelheim am Rhein, Germany), and then intubated and ventilated with isoflurane 2 % (Ecuphar Veterinaria, Barcelona, Cataluña, Spain). After topical administration of double anesthetic Colicursi® (0.1 % tetracaine and 0.4 % oxybuprocaine, Alcon, Geneva, Switzerland), a 4 mm incision was performed in the corneal tissue of the eye with a grooved knife in group 1 and a rGOM (area=4 mm^2) was introduced at the bottom of the stromal pocket. In group 2, an incision was made 3 mm from limbus separating conjunctiva and the capsule of Tenon and leaving the sclera exposed. Subsequently, a 2 mm scleral incision was performed and a rGOM (area=4 mm^2) was introduced. The scleral incision and the conjunctival tissue were closed with 6-0 vicryl suture (Ethicon, Bridgewater, New Jersey, USA). In both groups the contralateral eye remained as a healthy control. All rabbits were treated with topical antibiotic Tobrex® (3 mg/mL tobramycin, Alcon) applied every 12 h during the follow-up period.

The follow-up period was of 4 and 2 weeks in rabbits transplanted with intrastromal and intrascleral rGOM respectively. The exterior appearance of transplanted rabbit eyes was monitored by taking photographs once a week during the follow-up period and imaging studies with corneal and retinal optical coherence tomography (OCT) (Tomey, Nagoya, Aichi, Japan) were performed.

Finally, rabbits were euthanized by an intravenous overdose of pentobarbital sodium. The eyes were enucleated and fixed in 4 % paraformaldehyde for 24 h, embedded in paraffin, sectioned and stained with H/E and then analyzed under light microscopy.

2.6. *In vivo* genotoxicity of rGOM.

In vivo rGOM genotoxicity was examined in liver tissue of Wistar rats used for the *in vivo* biocompatibility assay. Briefly, hepatic tissue from animals euthanized at 21 days was washed 3 times with cold PBS. The tissue was then carefully chopped and incubated with trypsin/EDTA 0.25 % at 37°C for 30 min. After this time the sample was filtered through a Corning cell strainer® (Corning, New York, New York, USA) and the suspension was centrifuged at 400 rcf for 6 min. The obtained pellet was washed 3 times with PBS and finally resuspended in a volume of 2,500 µL of PBS. Finally, the comet assay was carried out as described above.

3. Results

3.1. Characterization of GO water suspension.

The statistical analysis of the AFM images indicated that the obtained GO had an average sheet height of 1.2 nm approximately. 60 % of the sheets showed sizes below 500 nm with a maximum population of sheets with size of ≈ 350 nm (Figure 1).

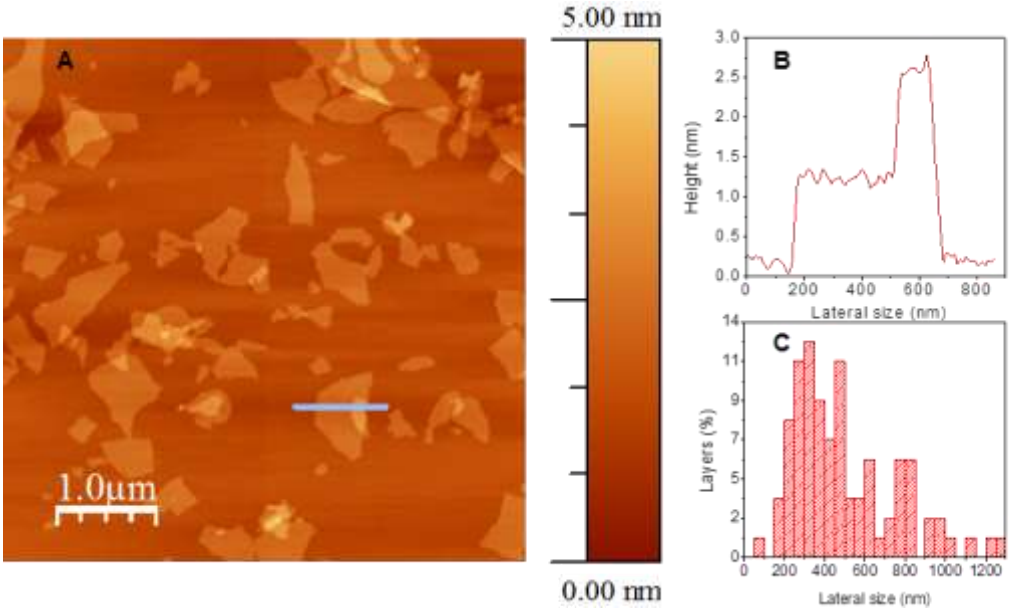

Figure 1. AFM image (A), height profile (B) and sheet size distribution (C) of GO water suspension.

3.2. Preparation and characterization of rGOM.

rGOM were obtained by evaporation of the GO water suspension and posterior chemical reduction of GO membranes by HI. The obtained rGOM resulted in flexible and easy to handle membranes with an area of 7 cm^2. SEM images showed a uniform and corrugated surface on both sides of the rGOM and a superposed multilayered structure through the cross-

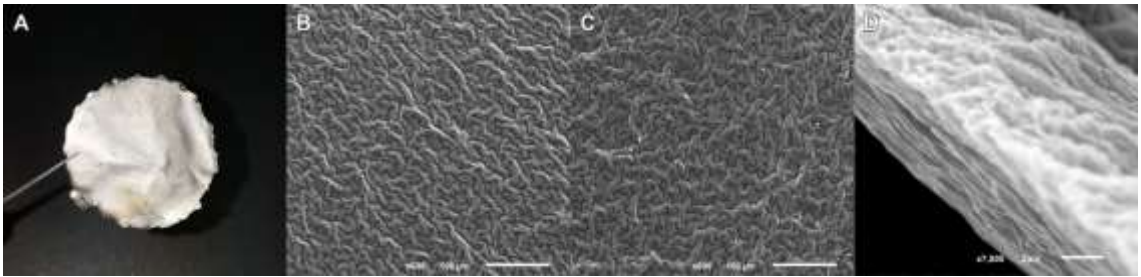

section of the rGOM (Figure 2).

Figure 2. Macrophotography of rGOM (A). SEM microphotographs of rGOM showing the surface of both sides of the membrane (B, C) and the cross-section (D).

The composition of rGOM and GO membranes was firstly analyzed by EDX (Table 1). As expected, rGOM showed a statistically significant decrease ($p<0.01$) in the oxygen content compared to GO membranes (23.45 and 46.34 wt%, respectively). The reducing agent (iodine) used in the preparation of rGOM was also detected (10.73 wt%). Furthermore, significant differences in the surface chemistry were also revealed by XPS (Table 1). The oxygen content in the surface of the rGOM was markedly lower than the measured in the raw membrane, which corroborated the removal of oxygenated functional groups through the reduction step. It is important to remark that no iodine content was measured as a result of the membranes pre-treatment required for this analysis.

Table 1. Chemical composition of rGOM and GO membranes.

SAMPLE	**EDX (wt. %)**			**XPS (at. %)**	
	C	**O**	**I**	**C**	**O**
rGOM	65.67	23.45	10.73	92.95	7.05
GO membranes	51.00	46.34	--	83.87	12.13

The electrical conductivity of GO and rGOM membranes were also analyzed. The chemical treatment with HI increased the conductivity of the GO membrane from 12.12 Sm^{-1} to $1.16x10^{5}$ Sm^{-1} in rGOM. This treatment also improved the mechanical properties of rGOM. The resistance, determined by burst strength showed an average value of 191.49 ± 28.02 g and the elasticity, determined by the distance at burst of 1.14 ± 0.12 mm. In both cases, the extreme fragility of GO membranes made it impossible to evaluate such parameters.

3.3. *In vitro* biocompatibility of rGOM.

By fluorescence microscopy and SEM, the different ocular cells analyzed were shown to attach when they were cultured on rGOM, maintaining their characteristic morphology. Thus, epithelial cell lines (ARPE-19 and HCE-T) were confluent at 48 h of culture showing a flat and polygonal morphology with positive stain for ZO-1 and RPE65 (ARPE-19) and E-cadherin and CK markers (HCE-T). Primary epithelial cells: corneal limbal cells and RPE, showed a rounder and polygonal morphology respectively. Corneal limbal cells began to migrate from limbal explant after 3 days of culture, and cells were confluent at 7 days showing positive stain for p63 and CK markers. RPE cells were cultured for 3 weeks while progressively reducing the percentage of FBS to 2 %. At that time, RPE cells showed ZO-1 and RPE65 positive staining. Finally, corneal keratocytes were confluent after 48 h of culture appearing as elongated cells staining positive for vimentin when they were cultured on rGOM. No apparent differences were found between rGOM and control group cultures (Figure 3).

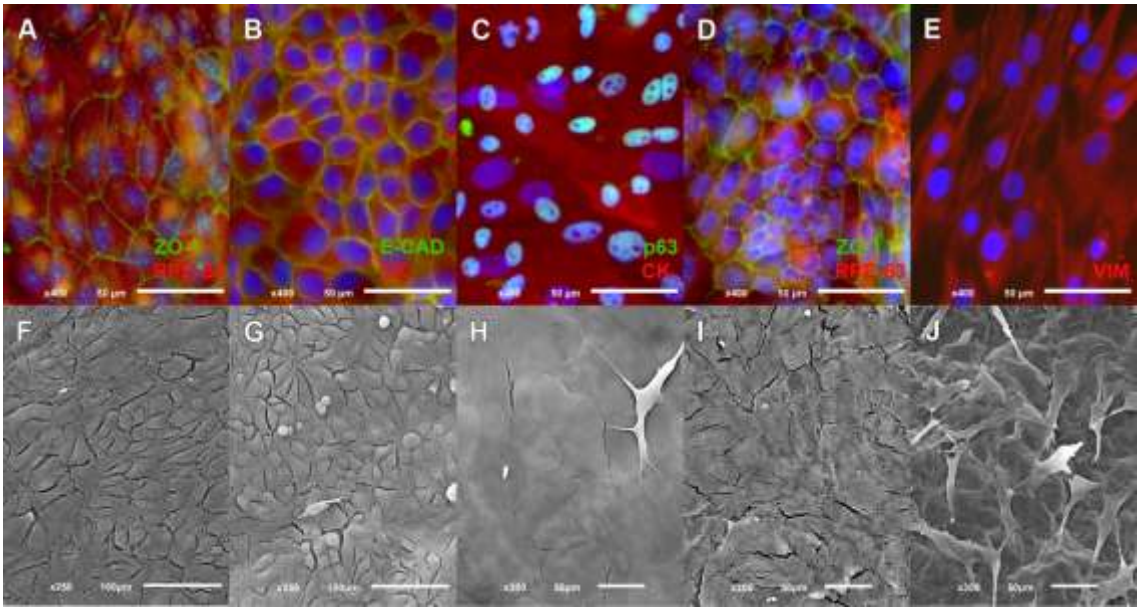

Figure 3. Immunofluorescence (A-E) and microphotographs of SEM (F-J) of ocular human cells cultured on rGOM: ARPE-19 (A, F), HCE-T (B, G), corneal limbal cells (C, H), RPE (D, I) and corneal keratocytes (E, J). Nuclei stained in blue.

3.4. *In vitro* genotoxicity assay.

The comet assay of cultured rGOM (Figure 4) revealed no statistically significant differences between the percentage of tail DNA in corneal keratocytes (13 ± 1.52 %) and ARPE-19 (11 ± 1.28 %) cultured on rGOM as compared to the same cells cultured on the conventional plastic (11 ± 0.9 %; 9 ± 0.92 %).

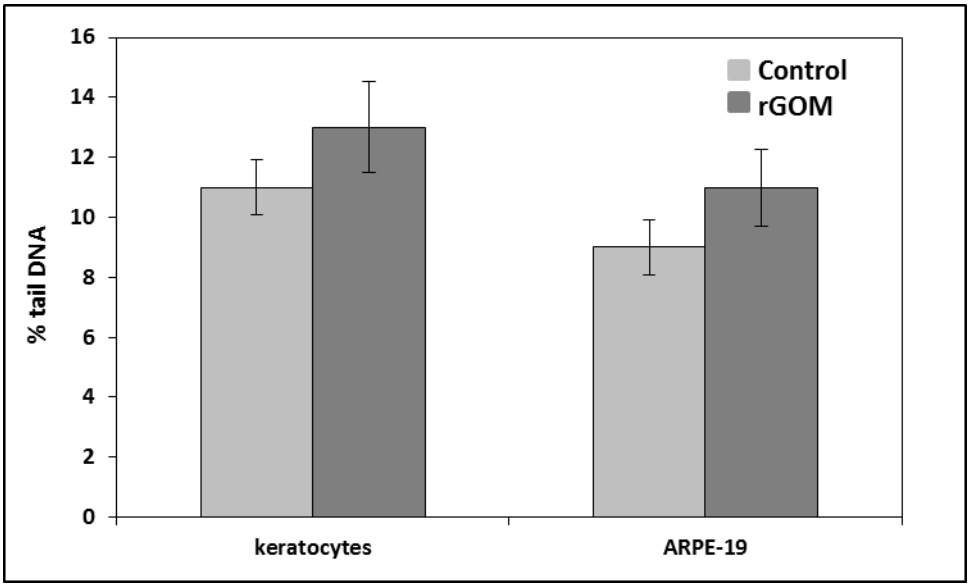

Figure 4. In vitro genotoxicity assay in corneal keratocytes and ARPE-19 after 48 h of culture on rGOM. Results (N=3) are shown as mean ± SEM.

3.5. *In vivo* biocompatibility of rGOM.

In vivo biocompatibility of rGOM in Wistar rats showed that the adjacent tissue to the subdermal implants had a healthy appearance without signs of inflammation or edema (Figure 5A and 5C). H/E histological analysis did not show any fibrotic tissue, macrophages, giant multinuclear cells or lymphoid infiltrates in the tissue adjacent to the implant at 7 days after surgery (Figure 5B). At 21 days, the subcutaneous graft showed a minimal fibrotic response in the tissue adjacent to the implant without lymphoid infiltrates (Figure 5D).

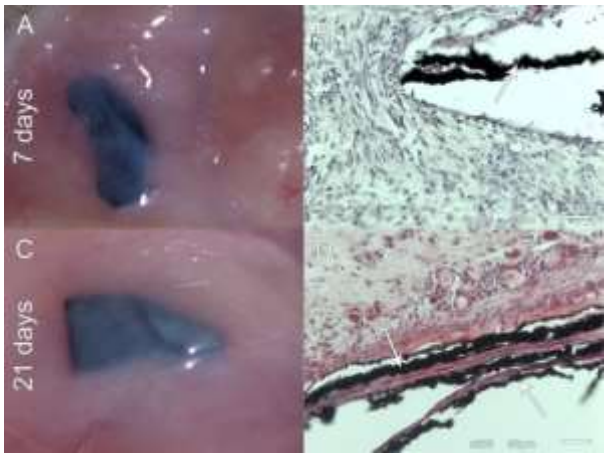

Figure 5. Macrophotographs (A, C) and H/E histological analysis (B, D) of rGOM implanted in the subdermal space of Wistar rats at 7 or 21 days of follow-up. rGOM is marked with arrows.

In vivo studies in rabbits showed good biocompatibility of rGOM in both groups: rabbits transplanted with intrastromal rGOM (group 1) and rabbits transplanted with intrascleral rGOM (group 2).

In group 1, rGOM was kept intact during the 4 weeks of the follow-up period. The OCT analysis showed that the structure of the cornea remained intact without any signs of alteration when compared to its healthy contralateral cornea. The histological sections of corneas transplanted with rGOM did not reveal evidence of macrophages, lymphoid infiltrate nor inflammatory response in the adjacent stromal tissue (Figure 6).

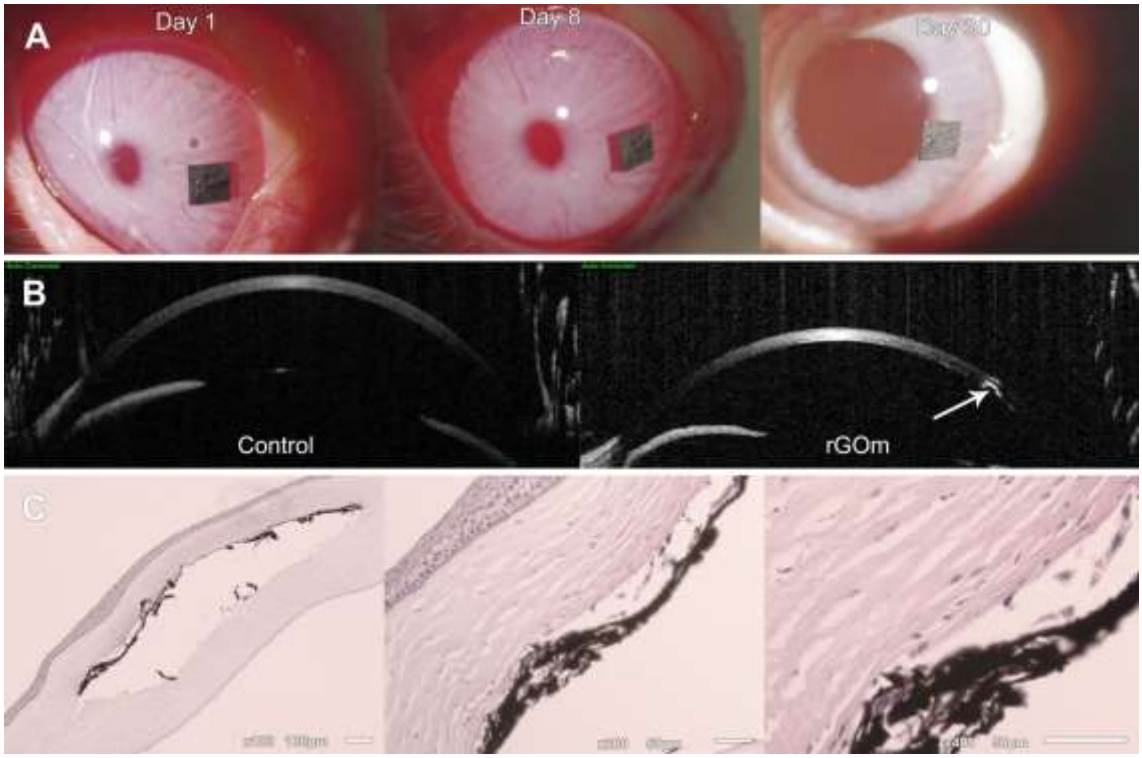

Figure 6. Macrophotographs (A), image of OCT (B) and H/E microphotographs (C) of intrastromal rGOM transplanted rabbits.

In group 2, rGOM was introduced in the scleral space without evidence of inflammation around the tissue adjacent to the implants. All rabbits preserved the integrity of inner and outer layers of the retina without associated retinal detachment (Figure 7).

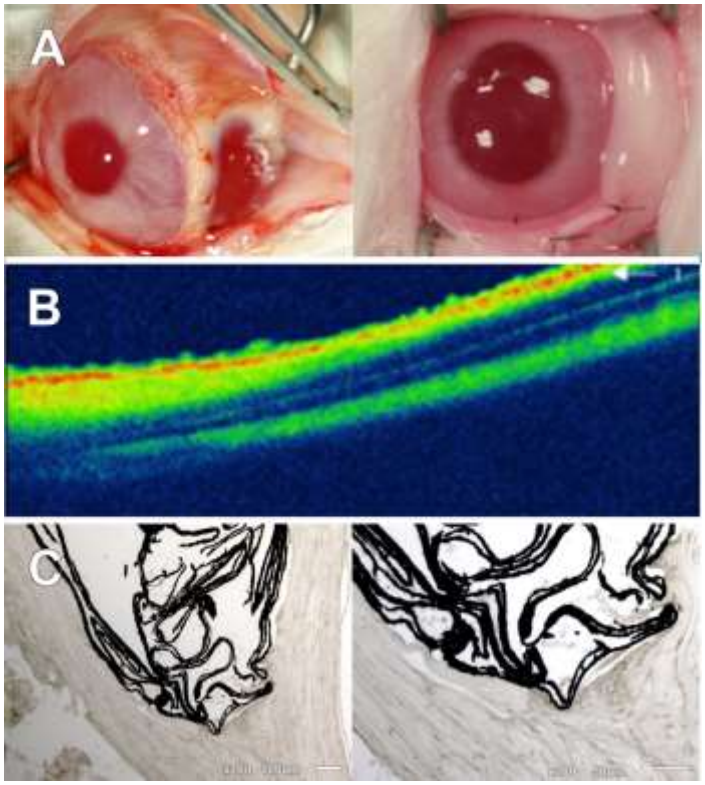

Figure 7. Macrophotographs (A), image of retinal OCT (B) and H/E microphotographs (C) of intrascleral rGOM transplanted rabbits.

All rabbits had a normal behavior and showed no signs of edema or ocular irritation during the follow-up period.

3.6. *In vivo* genotoxicity assay.

The comet assay of the hepatic tissue isolated from Wistar rats showed no statistically significant differences between rats transplanted with (8.96 ± 1.36 %) or without rGOM (9.61 ± 1.11 %), with the percentages of DNA in the tail similar in both groups.

4. Discussion

Since it was discovered in 2004 [56,57] graphene and its derivatives (GO and rGO) are one of the most promising materials in many industrial applications and more recently in Medicine. The development of graphene-based scaffolds for Regenerative Medicine or Tissue Engineering is a relatively new field with a promising future since several studies have demonstrated their capability in promoting cellular growth and the differentiation of several cell types without any toxic effect [58–60]. Moreover, its combination with other biomaterials provides excellent mechanical, physical and electrical properties allowing its use in cardiac, neural, bone, cartilage, skeletal muscle, skin or adipose Tissue Engineering [53,61].

Despite the potential applications of graphene, its toxic effect remains controversial [62] with several studies supporting its toxicity, while others show graphene as a biocompatible material. This is due to cytotoxicity and genotoxicity being related with its chemical functionality and the size of graphene sheets [25]. In this work, rGOM were developed from a GO water suspension, and *in vitro* and *in vivo* biocompatibility and

genotoxicity were studied with different types of ocular cells. Moreover, its integration upon implantation in dermal and ocular structures was also analyzed.

For the development of rGOM, a solution of GO was obtained from commercial graphite by the modified Hummer´s method [21]. The topological features of the GO water suspension revealed an average sheet height similar to those previously reported, indicating that the solution of GO was composed of single-layered graphene sheets [63].

There are different mechanical, chemical or thermal procedures for the preparation of graphene membranes [64]. In this study, we have developed a rGOM using an easy and simple procedure which consisted in the evaporation of a GO suspension in a laminar air flow cabinet. In accordance with previous studies [65], we firstly obtained GO membranes unsuitable for ocular applications, due to the degradation of the membranes upon contact with aqueous media. In order to solve this problem, GO membranes were subjected to reduction with HI, obtaining rGOM with a multilayered structure through the cross-section [66,67].

According to the EDX data, there was a decrease in the oxygen content after the reduction procedure in rGOM which is in accordance with the removal of oxygenated functional groups by the reducing agent [68]. Furthermore, significant differences in the surface chemistry were also revealed by XPS, and the oxygen content in the surface of the rGOM was markedly lower than the measured in the raw membrane. According to the literature, this result is directly related to the restoration of Csp^2 domains typical of graphene materials [69]. However, rGOM still retained a residual percentage of oxygen content, which could offer several advantages for its potential bioapplications [70].

The HI reduction process also improved the mechanical properties of rGOM making its use in surgical procedures possible. Moreover, it increased rGOM electrical conductivity as a consequence of the restoration of Csp2 domains when removing oxygenated functional groups. This property enlarges the use of graphene-based materials in ocular drug delivery therapies with a high level of temporal control and dosage flexibility [71]. Furthermore, electrical conductivity of graphene-based materials allows the growth of neuronal cells [26,72,73] and could modulate its behavior or differentiation, which may require bioelectrical signal transmissions [74], opening a new route for the development of a novel generation of flexible and high-sensitive neural prostheses [47,75,76].

In vitro studies showed that rGOM allowed the adhesion and growth of several ocular cell types. Two ocular cell lines, ARPE-19 and HCE-T were able to growth on rGOM while maintaining their shape and characteristic markers. In the same way primary cultures of retinal and corneal cells, representing a more physiological approach of ocular tissues, were cultured successfully on rGOM. These results demonstrated that graphene membranes did not have an *in vitro* cytotoxic effect.

However, assaying *in vitro* cytotoxicity does not truly represent the complexities of a living organism and its immune system, and thus cannot be assumed to be predictive of *in vivo* biocompatibility. For this reason, rGOM was studied upon implantation in Wistar rats, observing the absence of any acute inflammatory response when rGOM was transplanted in the subdermal space. There were no signs of inflammation in the adjacent tissue, as

subcutaneous muscle, adipose, and fascia layers appeared normal, indicating no acute or chronic cytotoxicity. These results are in synchrony with other studies performed on mice, where a suspension of GO was intravenously injected [77]. Finally, rGOM were used in intrastromal and intrascleral surgeries without any evidence of inflammation or cell toxicity in surrounding tissues, as seen by histological and tomography images, proving that rGOM could be used safely in ocular surgeries. These results are in accordance with several studies which had reported the biocompatibility of graphene or GO suspensions in these ocular spaces [48–50].

Since there are controversial studies about the *in vitro* and *in vivo* genotoxic effect of graphene [78,79], genotoxicity studies using the comet assay on alkaline conditions [80] were also performed in corneal and retinal cells. In our case, the results confirmed no significant differences between cells cultured on conventional plastic and cells cultured on rGOM. In the same way, hepatocytes of Wistar rats transplanted with subdermal rGOM did not shown DNA fragmentation when they were compared against control rat hepatocytes, which show that implanted rGOM did not induce DNA breakage genotoxicity at local and systemic level.

In Ophthalmology, several studies have initial focused in to prove the non-toxicity of GO and rGO suspensions [48,49,52] and develop medical devices [47] or graphene-based films [50]. Tissue Engineering techniques require scaffolds which provide mechanical support, chemical stimuli and biological signals to the cells. They also have to be non-toxic and easy to handle in a surgery.

In ocular Tissue Engineering, scaffolds should meet the same criteria, but if the scaffold is grafted in the visual line (central part of the cornea and lens, pupil or central part of the vitreous) it must also to be optically transparent. In recent years, ocular Regenerative Medicine has moved towards the development of several membranes with these characteristics. Amniotic membrane [34,81], gelatin [82,83], silk fibroin [84–86] and collagen membranes [38,39] have already proved their value for treating different ocular disorders in the clinical practice or experimental research. Although the optical properties of rGOM could make it unsuitable for certain corneal applications, others characteristics such as its non-toxicity, surgical manageability and its possible antibacterial properties, make it a promising membrane for its use in applications in which the scaffold is grafted out of the visual line, in retinal surgery or when the graft is removed several days after implantation.

Although the results obtained in this study are very promising, the follow-up period was too short to determine if rGOM can be used without causing adverse long-term effects. Furthermore, more in vivo studies could be realized to determine if rGOM is certainly a scaffold suitable in the treatment of ocular diseases.

In this study, rGOM was not subjected to any final sterilization process prior to the cellular analysis. Despite this, we did not find any bacterial contamination during the culture period. It is possible that the Hummers' method (which involve high temperatures and low pH) used to produce GO sterilized the material [87]. However, the subsequent processing steps were not performed in aseptic conditions, suggesting that rGOM could retain the antibacterial properties of graphene [20] during the cell culture. In our opinion, if rGOM maintains this

property when is grafted, this could be an advantage of rGOM compared to others types of scaffolds which are very sensible to infections when they are grafted.

5. Conclusion

In this study, we developed a reduced graphene oxide membrane (rGOM) which allowed the growth of different ocular cells by using a simple and easy procedure of air drying and chemical reduction starting from a GO water suspension. Moreover, this membrane did not induce *in vitro* or *in vivo* cytotoxicity or genotoxicity in the short-term follow-up. These results suggest that rGOM may be used in Ophthalmology as scaffold for cell-based therapies.

Acknowledgements: Authors wish to thank the team from Centro Comunitario de Sangre y Tejidos de Asturias for their skillful technical assistance.

References:

[1] Y. Zhang, L. Zhang, C. Zhou, Review of chemical vapor deposition of graphene and related applications, Acc. Chem. Res. 46 (2013) 2329–2339. https://doi.org/10.1021/ar300203n.

[2] L. Yan, Y.B. Zheng, F. Zhao, S. Li, X. Gao, B. Xu, P.S. Weiss, Y. Zhao, Chemistry and physics of a single atomic layer: Strategies and challenges for functionalization of graphene and graphene-based materials, Chem. Soc. Rev. 41 (2012) 97–114. https://doi.org/10.1039/c1cs15193b.

[3] K. Yang, L. Feng, X. Shi, Z. Liu, Nano-graphene in biomedicine: Theranostic applications, Chem. Soc. Rev. 42 (2013) 530–547. https://doi.org/10.1039/c2cs35342c.

[4] P.T. Yin, S. Shah, M. Chhowalla, K.B. Lee, Design, synthesis, and characterization of graphene-nanoparticle hybrid materials for bioapplications, Chem. Rev. 115 (2015) 2483–2531. https://doi.org/10.1021/cr500537t.

[5] J.S. Lee, J. Oh, J. Jun, J. Jang, Wireless Hydrogen Smart Sensor Based on Pt/Graphene-Immobilized Radio-Frequency Identification Tag, ACS Nano. 9 (2015) 7783–7790. https://doi.org/10.1021/acsnano.5b02024.

[6] E.J. Yoo, J. Kim, E. Hosono, H.S. Zhou, T. Kudo, I. Honma, Large reversible Li storage of graphene nanosheet families for use in rechargeable lithium ion batteries, Nano Lett. 8 (2008) 2277–2282. https://doi.org/10.1021/nl800957b.

[7] L. Huang, Z. Zhang, Z. Li, B. Chen, X. Ma, L. Dong, L.-M. Peng, Multifunctional graphene sensors for magnetic and hydrogen detection, ACS Appl. Mater. Interfaces. 7 (2015) 9581–9588. https://doi.org/10.1021/acsami.5b01070.

[8] R. Messina, P. Ben-Abdallah, Graphene-based photovoltaic cells for near-field thermal energy conversion, Sci. Rep. 3 (2013) 1383. https://doi.org/10.1038/srep01383.

[9] Y. Liu, D. Yu, C. Zeng, Z. Miao, L. Dai, Biocompatible graphene oxide-based glucose biosensors, Langmuir. 26 (2010) 6158–6160. https://doi.org/10.1021/la100886x.

[10] C.H. Lu, H.H. Yang, C.L. Zhu, X. Chen, G.N. Chen, A Graphene Platform for Sensing Biomolecules, Angew. Chemie Int. Ed. 48 (2009) 4785–4787. https://doi.org/10.1002/anie.200901479.

[11] Y. Xia, Nanomaterials at work in biomedical research, Nat. Mater. 7 (2008) 758–760. https://doi.org/10.1038/nmat2277.

[12] X. Sun, Z. Liu, K. Welsher, J.T. Robinson, A. Goodwin, S. Zaric, H. Dai, Nano-graphene oxide for cellular imaging and drug delivery, Nano Res. 1 (2008) 203–212. https://doi.org/10.1007/s12274-008-8021-8.

[13] M. Shahabi, H. Raissi, Screening of the structural, topological, and electronic properties of the functionalized Graphene nanosheets as potential Tegafur anticancer drug carriers using DFT method, J. Biomol. Struct. Dyn. 36 (2018) 2517–2529. https://doi.org/10.1080/07391102.2017.1360209.

[14] H. Shen, L. Zhang, M. Liu, Z. Zhang, Biomedical applications of graphene, Theranostics. 2 (2012) 283–294. https://doi.org/10.7150/thno.3642.

[15] W. Zhang, Z. Guo, D. Huang, Z. Liu, X. Guo, H. Zhong, Synergistic effect of chemo-photothermal therapy using PEGylated graphene oxide, Biomaterials. 32 (2011) 8555–8561. https://doi.org/10.1016/j.biomaterials.2011.07.071.

[16] P. Huang, C. Xu, J. Lin, C. Wang, X. Wang, C. Zhang, X. Zhou, S. Guo, D. Cui, Folic Acid-conjugated Graphene Oxide loaded with Photosensitizers for Targeting Photodynamic Therapy, Theranostics. 1 (2011) 240–250. https://doi.org/10.7150/thno/v01p0240.

[17] S. Gurunathan, J.W. Han, A. Abdal Dayem, V. Eppakayala, J.H. Kim, Oxidative stress-mediated antibacterial activity of graphene oxide and reduced graphene oxide in Pseudomonas aeruginosa, Int. J. Nanomedicine. 7 (2012) 5901–5914. https://doi.org/10.2147/IJN.S37397.

[18] J. Chen, H. Peng, X. Wang, F. Shao, Z. Yuan, H. Han, Graphene oxide exhibits broad-spectrum antimicrobial activity against bacterial phytopathogens and fungal conidia by intertwining and membrane perturbation, Nanoscale. 6 (2014) 1879–1889. https://doi.org/10.1039/c3nr04941h.

[19] F. Perreault, A.F. De Faria, S. Nejati, M. Elimelech, Antimicrobial Properties of Graphene Oxide Nanosheets: Why Size Matters, ACS Nano. 9 (2015) 7226–7236. https://doi.org/10.1021/acsnano.5b02067.

[20] W. Hu, C. Peng, W. Luo, M. Lv, X. Li, D. Li, Q. Huang, C. Fan, Graphene-based antibacterial paper, ACS Nano. 4 (2010) 4317–4323. https://doi.org/10.1021/nn101097v.

[21] W.S. Hummers, R.E. Offeman, Preparation of Graphitic Oxide, J. Am. Chem. Soc. 80 (1958) 1339. https://doi.org/10.1021/ja01539a017.

[22] X. Huang, Z. Yin, S. Wu, X. Qi, Q. He, Q. Zhang, Q. Yan, F. Boey, H. Zhang, Graphene-based materials: Synthesis, characterization, properties, and applications, Small. 7 (2011) 1876–1902. https://doi.org/10.1002/smll.201002009.

[23] S. Park, R.S. Ruoff, Chemical methods for the production of graphenes, Nat. Nanotechnol. 4 (2009) 217–224. https://doi.org/10.1038/nnano.2009.58.

[24] C. Botas, P. Álvarez, P. Blanco, M. Granda, C. Blanco, R. Santamaría, L.J. Romasanta, R. Verdejo, M.A. López-Manchado, R. Menéndez, Graphene materials with different structures prepared from the same graphite by the Hummers and Brodie methods, Carbon N. Y. 65 (2013) 156–164. https://doi.org/10.1016/j.carbon.2013.08.009.

[25] K. Kostarelos, K.S. Novoselov, Exploring the interface of graphene and biology, Science. 344 (2014) 261–263. https://doi.org/10.1126/science.1246736.

[26] N. Li, X. Zhang, Q. Song, R. Su, Q. Zhang, T. Kong, L. Liu, G. Jin, M. Tang, G. Cheng, The promotion of neurite sprouting and outgrowth of mouse hippocampal cells in culture by graphene substrates, Biomaterials. 32 (2011) 9374–9382. https://doi.org/10.1016/j.biomaterials.2011.08.065.

[27] H. Ali-Boucetta, D. Bitounis, R. Raveendran-Nair, A. Servant, J. Van den Bossche, K. Kostarelos, Purified Graphene Oxide Dispersions Lack In Vitro Cytotoxicity and In Vivo Pathogenicity, Adv. Healthc. Mater. 2 (2013) 433–441. https://doi.org/10.1002/adhm.201200248.

[28] J.H. Liu, S.T. Yang, H. Wang, Y. Chang, A. Cao, Y. Liu, Effect of size and dose on the biodistribution of graphene oxide in mice, Nanomedicine. 7 (2012) 1801–1812. https://doi.org/10.2217/nnm.12.60.

[29] D. Sahni, A. Jea, J.A. Mata, D.C. Marcano, A. Sivaganesan, J.M. Berlin, C.E. Tatsui, Z. Sun, T.G. Luerssen, S. Meng, T.A. Kent, J.M. Tour, Biocompatibility of pristine graphene for neuronal interface: Laboratory investigation, J. Neurosurg. Pediatr. 11 (2013) 575–583. https://doi.org/10.3171/2013.1.PEDS12374.

[30] N.V.S. Vallabani, S. Mittal, R.K. Shukla, A.K. Pandey, S.R. Dhakate, R. Pasricha, A. Dhawan, Toxicity of graphene in normal human lung cells (BEAS-2B), J. Biomed. Nanotechnol. 7 (2011) 106–107. https://doi.org/10.1166/jbn.2011.1224.

[31] K.H. Liao, Y.S. Lin, C.W. MacOsko, C.L. Haynes, Cytotoxicity of graphene oxide and graphene in human erythrocytes and skin fibroblasts, ACS Appl. Mater. Interfaces. 3 (2011) 2607–2615. https://doi.org/10.1021/am200428v.

[32] Y. Zhang, S.F. Ali, E. Dervishi, Y. Xu, Z. Li, D. Casciano, A.S. Biris, Cytotoxicity effects of graphene and single-wall carbon nanotubes in neural phaeochromocytoma-derived pc12 cells, ACS Nano. 4 (2010) 3181–3186. https://doi.org/10.1021/nn1007176.

[33] W. Hu, C. Peng, M. Lv, X. Li, Y. Zhang, N. Chen, C. Fan, Q. Huang, Protein corona-mediated mitigation of cytotoxicity of graphene oxide, ACS Nano. 5 (2011) 3693–3700. https://doi.org/10.1021/nn200021j.

[34] A.K. Riau, R.W. Beuerman, L.S. Lim, J.S. Mehta, Preservation, sterilization and de-epithelialization of human amniotic membrane for use in ocular surface reconstruction, Biomaterials. 31 (2010) 216–225. https://doi.org/10.1016/j.biomaterials.2009.09.034.

[35] S. Burman, S. Tejwani, G.K. Vemuganti, U. Gopinathan, V.S. Sangwan, Ophthalmic applications of preserved human amniotic membrane: A review of current indications, Cell Tissue Bank. 5 (2004) 161–175. https://doi.org/10.1023/B:CATB.0000046067.25057.0a.

[36] P. Rama, G. Ferrari, G. Pellegrini, Cultivated limbal epithelial transplantation, Curr. Opin. Ophthalmol. 28 (2017) 387–389. https://doi.org/10.1097/ICU.0000000000000382.

[37] L. Liang, H. Sheha, J. Li, S.C.G. Tseng, Limbal stem cell transplantation: new progresses and challenges, Eye (Lond). 23 (2009) 1946–1953. https://doi.org/10.1038/eye.2008.379.

[38] T. Mimura, S. Yamagami, S. Yokoo, T. Usui, K. Tanaka, S. Hattori, S. Irie, K. Miyata, M.

Araie, S. Amano, Cultured human corneal endothelial cell transplantation with a collagen sheet in a rabbit model, Investig. Ophthalmol. Vis. Sci. 45 (2004) 2992–2997. https://doi.org/10.1167/iovs.03-1174.

[39] N. Vázquez, M. Chacó N, C. a Rodríguez-Barrientos, J.S. Merayo-Lloves, M. Naveiras, B. Baamonde, J.F. Alfonso, I. Zambrano-Andazol, A.C. Riestra, L. Meana, Human Bone Derived Collagen for the Development of an Artificial Corneal Endothelial Graft. In Vivo Results in a Rabbit Model, (2016) 1–18. https://doi.org/10.1371/journal.pone.0167578.

[40] D. Tsoukanas, P. Xanthopoulou, A.C. Charonis, P. Theodossiadis, G. Kopsinis, T. Filippopoulos, Heterologous, Fresh, Human Donor Sclera as Patch Graft Material in Glaucoma Drainage Device Surgery, J. Glaucoma. 25 (2016) 558–564. https://doi.org/10.1097/IJG.0000000000000294.

[41] J.D. Arias, A.T. Hoyos, B. Alcántara, R.M. Sanchez-Avila, F.J. Arango, V. Galvis, PLASMA RICH IN GROWTH FACTORS FOR PERSISTENT MACULAR HOLE, Retin. Cases Brief Rep. (2019) 1. https://doi.org/10.1097/icb.0000000000000957.

[42] R.M. Sánchez-ávila, Á.F.V. González, Á.F.V. Sanz, J. Merayo-Lloves, Treatment of recurrent myopic macular hole using membrane of plasma rich in growth factors, Int. Med. Case Rep. J. 12 (2019) 229–233. https://doi.org/10.2147/IMCRJ.S170329.

[43] S. Lee, I. Jo, S. Kang, B. Jang, J. Moon, J.B. Park, S. Lee, S. Rho, Y. Kim, B.H. Hong, Smart Contact Lenses with Graphene Coating for Electromagnetic Interference Shielding and Dehydration Protection, ACS Nano. 11 (2017) 5318–5324. https://doi.org/10.1021/acsnano.7b00370.

[44] K. Choi, H.G. Park, Smart Reinvention of the Contact Lens with Graphene, ACS Nano. 11 (2017) 5223–5226. https://doi.org/10.1021/acsnano.7b03180.

[45] J.F. Huang, J. Zhong, G.P. Chen, Z.T. Lin, Y. Deng, Y.L. Liu, P.Y. Cao, B. Wang, Y. Wei, T. Wu, J. Yuan, G.B. Jiang, A Hydrogel-Based Hybrid Theranostic Contact Lens for Fungal Keratitis, ACS Nano. 10 (2016) 6464–6473. https://doi.org/10.1021/acsnano.6b00601.

[46] M. Sinha, T. Gupte, Design and evaluation of artificial cornea with core–skirt design using polyhydroxyethyl methacrylate and graphite, Int. Ophthalmol. 38 (2018) 1225–1233. https://doi.org/10.1007/s10792-017-0586-3.

[47] J.W. Yang, M.L. Tseng, Y.M. Fu, C.H. Kang, Y.T. Cheng, P.H. Kuo, C.K. Tzeng, S.H. Chiou, C.Y. Wu, G.Y. Chen, Printable Graphene Oxide Micropatterns for a Bio-Subretinal Chip, Adv. Healthc. Mater. 7 (2018) e1800365. https://doi.org/10.1002/adhm.201800365.

[48] L. Yan, Y. Wang, X. Xu, C. Zeng, J. Hou, M. Lin, J. Xu, F. Sun, X. Huang, L. Dai, F. Lu, Y. Liu, Can graphene oxide cause damage to eyesight?, Chem. Res. Toxicol. 25 (2012) 1265–1270. https://doi.org/10.1021/tx300129f.

[49] M. Lin, R. Zou, H. Shi, S. Yu, X. Li, R. Guo, L. Yan, G. Li, Y. Liu, L. Dai, Ocular biocompatibility evaluation of hydroxyl-functionalized graphene, Mater. Sci. Eng. C. 50 (2015) 300–308. https://doi.org/10.1016/j.msec.2015.01.086.

[50] X.W. Tan, B. Thompson, A. Konstantopoulos, T.W. Goh, M. Setiawan, G.H.F. Yam, D. Tan, K.A. Khor, J.S. Mehta, Application of graphene as candidate biomaterial for synthetic keratoprosthesis skirt, Investig. Ophthalmol. Vis. Sci. 56 (2015) 6605–6611. https://doi.org/10.1167/iovs.15-17306.

[51] W. Wu, L. Yan, Q. Wu, Y. Li, Q. Li, S. Chen, Y. Yang, Z. Gu, H. Xu, Z.Q. Yin, Evaluation of the toxicity of graphene oxide exposure to the eye, Nanotoxicology. 10 (2016) 1329–1340. https://doi.org/10.1080/17435390.2016.1210692.

[52] W. An, Y. Zhang, X. Zhang, K. Li, Y. Kang, S. Akhtar, X. Sha, L. Gao, Ocular toxicity of reduced graphene oxide or graphene oxide exposure in mouse eyes, Exp. Eye Res. 174 (2018) 59–69. https://doi.org/10.1016/j.exer.2018.05.024.

[53] S.R. Shin, Y.C. Li, H.L. Jang, P. Khoshakhlagh, M. Akbari, A. Nasajpour, Y.S. Zhang, A. Tamayol, A. Khademhosseini, Graphene-based materials for tissue engineering, Adv. Drug Deliv. Rev. 105 (2016) 255–274. https://doi.org/10.1016/j.addr.2016.03.007.

[54] R.G. Bai, K. Muthoosamy, S. Manickam, A. Hilal-Alnaqbi, Graphene-based 3D scaffolds in tissue engineering: Fabrication, applications, and future scope in liver tissue engineering, Int. J. Nanomedicine. 14 (2019) 5753–5783. https://doi.org/10.2147/IJN.S192779.

[55] N.P. Singh, M.T. McCoy, R.R. Tice, E.L. Schneider, A simple technique for quantitation of low levels of DNA damage in individual cells, Exp. Cell Res. 175 (1988) 184–191. https://doi.org/10.1016/0014-4827(88)90265-0.

[56] K.S. Novoselov, A.K. Geim, S. V. Morozov, D. Jiang, Y. Zhang, S. V. Dubonos, I. V. Grigorieva, A.A. Firsov, Electric field in atomically thin carbon films, Science. 306 (2004) 666–669. https://doi.org/10.1126/science.1102896.

[57] A.K. Geim, K.S. Novoselov, The rise of graphene, Nat. Mater. 6 (2007) 183–191. https://doi.org/10.1038/nmat1849.

[58] S. Agarwal, X. Zhou, F. Ye, Q. He, G.C.K. Chen, J. Soo, F. Boey, H. Zhang, P. Chen, Interfacing live cells with nanocarbon substrates, Langmuir. 26 (2010) 2244–2247. https://doi.org/10.1021/la9048743.

[59] N. Li, Q. Zhang, S. Gao, Q. Song, R. Huang, L. Wang, L. Liu, J. Dai, M. Tang, G. Cheng, Three-dimensional graphene foam as a biocompatible and conductive scaffold for neural stem cells, Sci. Rep. 3 (2013) 1604. https://doi.org/10.1038/srep01604.

[60] S.H. Ku, C.B. Park, Myoblast differentiation on graphene oxide, Biomaterials. 34 (2013) 2017–2023. https://doi.org/10.1016/j.biomaterials.2012.11.052.

[61] S. Han, J. Sun, S. He, M. Tang, R. Chai, The application of graphene-based biomaterials in biomedicine, Am. J. Transl. Res. 11 (2019) 3246–3260.

[62] A.M. Pinto, I.C. Gonçalves, F.D. Magalhães, Graphene-based materials biocompatibility: A review, Colloids Surfaces B Biointerfaces. 111 (2013) 188–202. https://doi.org/10.1016/j.colsurfb.2013.05.022.

[63] C. Botas, A.M. Pérez-Mas, P. Álvarez, R. Santamaría, M. Granda, C. Blanco, R. Menéndez, Optimization of the size and yield of graphene oxide sheets in the exfoliation step, Carbon N. Y. 63 (2013) 576–578. https://doi.org/10.1016/j.carbon.2013.06.096.

[64] H.W. Yoon, Y.H. Cho, H.B. Park, Graphene-based membranes: Status and prospects, Philos. Trans. R. Soc. A Math. Phys. Eng. Sci. 374 (2016) 20150024. https://doi.org/10.1098/rsta.2015.0024.

[65] M.C. Serrano, J. Patiño, C. García-Rama, M.L. Ferrer, J.L.G. Fierro, A. Tamayo, J.E. Collazos-Castro, F. Del Monte, M.C. Gutiérrez, 3D free-standing porous scaffolds made of graphene oxide as substrates for neural cell growth, J. Mater. Chem. B. 2 (2014) 5698–5706. https://doi.org/10.1039/c4tb00652f.

[66] S. Park, N. Mohanty, J.W. Suk, A. Nagaraja, J. An, R.D. Piner, W. Cai, D.R. Dreyer, V. Berry, R.S. Ruoff, Biocompatible, robust free-standing paper composed of a TWEEN/graphene composite, Adv. Mater. 22 (2010) 1736–1740. https://doi.org/10.1002/adma.200903611.

[67] D.A. Dikin, S. Stankovich, E.J. Zimney, R.D. Piner, G.H.B. Dommett, G. Evmenenko, S.T. Nguyen, R.S. Ruoff, Preparation and characterization of graphene oxide paper, Nature. 448 (2007) 457–460. https://doi.org/10.1038/nature06016.

[68] Z. González, C. Flox, C. Blanco, M. Granda, J.R. Morante, R. Menéndez, R. Santamaría, Outstanding electrochemical performance of a graphene-modified graphite felt for vanadium redox flow battery application, J. Power Sources. 338 (2017) 155–162. https://doi.org/10.1016/j.jpowsour.2016.10.069.

[69] Z. González, C. Botas, C. Blanco, R. Santamaría, M. Granda, P. Álvarez, R. Menéndez, Thermally reduced graphite and graphene oxides in VRFBs, Nano Energy. 2 (2013) 1322–1328. https://doi.org/10.1016/j.nanoen.2013.06.014.

[70] D. Chen, L. Tang, J. Li, Graphene-based materials in electrochemistry, Chem. Soc. Rev. 39 (2010) 3157–3180. https://doi.org/10.1039/b923596e.

[71] C.L. Weaver, J.M. Larosa, X. Luo, X.T. Cui, Electrically controlled drug delivery from graphene oxide nanocomposite films, ACS Nano. 8 (2014) 1834–1843. https://doi.org/10.1021/nn406223e.

[72] Q. Tu, L. Pang, Y. Chen, Y. Zhang, R. Zhang, B. Lu, J. Wang, Effects of surface charges of graphene oxide on neuronal outgrowth and branching, Analyst. 139 (2014) 105–115. https://doi.org/10.1039/c3an01796f.

[73] S.Y. Park, J. Park, S.H. Sim, M.G. Sung, K.S. Kim, B.H. Hong, S. Hong, Enhanced differentiation of human neural stem cells into neurons on graphene, Adv. Mater. 23 (2011) H263–H267. https://doi.org/10.1002/adma.201101503.

[74] S.K. Lee, H. Kim, B.S. Shim, Graphene: an emerging material for biological tissue engineering, Carbon Lett. 14 (2013) 63–75. https://doi.org/10.5714/cl.2013.14.2.063.

[75] A. Bendali, L.H. Hess, M. Seifert, V. Forster, A.F. Stephan, J.A. Garrido, S. Picaud, Purified Neurons can Survive on Peptide-Free Graphene Layers, Adv. Healthc. Mater. 2 (2013) 929–933. https://doi.org/10.1002/adhm.201200347.

[76] C.H. Chen, C. Te Lin, W.L. Hsu, Y.C. Chang, S.R. Yeh, L.J. Li, D.J. Yao, A flexible hydrophilic-modified graphene microprobe for neural and cardiac recording, Nanomedicine Nanotechnology, Biol. Med. 9 (2013) 600–604. https://doi.org/10.1016/j.nano.2012.12.004.

[77] H. Wu, H. Shi, Y. Wang, X. Jia, C. Tang, J. Zhang, S. Yang, Hyaluronic acid conjugated graphene oxide for targeted drug delivery, Carbon N. Y. 69 (2014) 379–389. https://doi.org/10.1016/j.carbon.2013.12.039.

[78] M. Hinzmann, S. Jaworski, M. Kutwin, J. Jagiełło, R. Koziński, M. Wierzbicki, M. Grodzik,

L. Lipińska, E. Sawosz, A. Chwalibog, Nanoparticles containing allotropes of carbon have genotoxic effects on glioblastoma multiforme cells, Int. J. Nanomedicine. 9 (2014) 2409–2417. https://doi.org/10.2147/IJN.S62497.

[79] S. Bengtson, K. Kling, A.M. Madsen, A.W. Noergaard, N.R. Jacobsen, P.A. Clausen, B. Alonso, A. Pesquera, A. Zurutuza, R. Ramos, H. Okuno, J. Dijon, H. Wallin, U. Vogel, No cytotoxicity or genotoxicity of graphene and graphene oxide in murine lung epithelial FE1 cells in vitro, Environ. Mol. Mutagen. 57 (2016) 469–482. https://doi.org/10.1002/em.22017.

[80] M. Espina, M. Corte-Rodríguez, L. Aguado, M. Montes-Bayón, M.I. Sierra, P. Martínez-Camblor, E. Blanco-González, L.M. Sierra, Cisplatin resistance in cell models evaluation of metallomic and biological predictive biomarkers to address early therapy failure, Metallomics. 9 (2017) 564–574. https://doi.org/10.1039/c7mt00014f.

[81] Y. Ishino, Y. Sano, T. Nakamura, C.J. Connon, H. Rigby, N.J. Fullwood, S. Kinoshita, Amniotic membrane as a carrier for cultivated human corneal endothelial cell transplantation, Investig. Ophthalmol. Vis. Sci. 45 (2004) 800–806. https://doi.org/10.1167/iovs.03-0016.

[82] M.M. Jumblatt, D.M. Maurice, B.D. Schwartz, A gelatin membrane substrate for the transplantation of tissue cultured cells, Transplantation. 29 (1980) 498–499. https://doi.org/10.1097/00007890-198006000-00013.

[83] J.-Y. Lai, K.-H. Chen, G.-H. Hsiue, Tissue-engineered human corneal endothelial cell sheet transplantation in a rabbit model using functional biomaterials, Transplantation. 84 (2007) 1222–1232. https://doi.org/10.1097/01.tp.0000287336.09848.39.

[84] P.W. Madden, J.N.X. Lai, K.A. George, T. Giovenco, D.G. Harkin, T. V. Chirila, Human corneal endothelial cell growth on a silk fibroin membrane, Biomaterials. 32 (2011) 4076–4084. https://doi.org/10.1016/j.biomaterials.2010.12.034.

[85] K. Higa, N. Takeshima, F. Moro, T. Kawakita, M. Kawashima, M. Demura, J. Shimazaki, T. Asakura, K. Tsubota, S. Shimmura, Porous silk fibroin film as a transparent carrier for cultivated corneal epithelial sheets, J. Biomater. Sci. Polym. Ed. 22 (2011) 2261–2276. https://doi.org/10.1163/092050610X538218.

[86] N. Vázquez, C.A. Rodríguez-Barrientos, S.D. Aznar-Cervantes, M. Chacón, J.L. Cenis, A.C. Riestra, R.M. Sánchez-Avila, M. Persinal, A. Brea-Pastor, L. Fernández-Vega Cueto, Á. Meana, J. Merayo-Lloves, Silk fibroin films for corneal endothelial regeneration: Transplant in a rabbit descemet membrane endothelial keratoplasty, Investig. Ophthalmol. Vis. Sci. 58 (2017) 3357–3365. https://doi.org/10.1167/iovs.17-21797.

[87] A.F. Rodrigues, L. Newman, N. Lozano, S.P. Mukherjee, B. Fadeel, C. Bussy, K. Kostarelos, A blueprint for the synthesis and characterisation of thin graphene oxide with controlled lateral dimensions for biomedicine, 2D Mater. 5 (2018) 035020. https://doi.org/10.1088/2053-1583/aac05c.